



**HAL**  
open science

## Identification of the state of suspension elements in railway systems

Ronald Martinod, German René Betancur, Leonel F Castañeda

► **To cite this version:**

Ronald Martinod, German René Betancur, Leonel F Castañeda. Identification of the state of suspension elements in railway systems. *Vehicle System Dynamics*, 2012, 50 (7), pp.1121-1135. 10.1080/00423114.2012.656657. hal-02182242

**HAL Id: hal-02182242**

**<https://hal.science/hal-02182242>**

Submitted on 16 Jul 2019

**HAL** is a multi-disciplinary open access archive for the deposit and dissemination of scientific research documents, whether they are published or not. The documents may come from teaching and research institutions in France or abroad, or from public or private research centers.

L'archive ouverte pluridisciplinaire **HAL**, est destinée au dépôt et à la diffusion de documents scientifiques de niveau recherche, publiés ou non, émanant des établissements d'enseignement et de recherche français ou étrangers, des laboratoires publics ou privés.



**Identification of the technical state of suspension elements  
in railway systems**

Journal:	<i>Vehicle System Dynamics</i>
Manuscript ID:	NVSD-2011-0096
Manuscript Type:	Original Paper
Date Submitted by the Author:	04-May-2011
Complete List of Authors:	Castañeda, Leonel; EAFIT University, Mechanical Engineering Martinod, Ronald; EAFIT University, Mechanical Engineering Betancur, German; EAFIT University, Mechanical Engineering
Keywords:	IRF, LSCE, OMA, multi-body model, railway testing, stabilization diagram

SCHOLARONE™  
Manuscripts

## Identification of the state of suspension elements in railway systems

R.M. Martinod<sup>a</sup>, G.R. Betancur<sup>a</sup> y L.F. Castañeda<sup>a\*</sup>

*<sup>a</sup>Mechanical Engineering Department, GEMI Research Group, EAFIT University, Medellín, Colombia*

Ronald Mauricio Martinod<sup>a</sup>

E.mail: [rmartino@eafit.edu.co](mailto:rmartino@eafit.edu.co)

Adress: Carrera 49 N° 7 Sur 50 of. 14-203, Medellín (Colombia – South America)

Phone number: (57) (4) - 261 95 00 ext. 9896

Germán René Betancur<sup>a</sup>

E.mail: [gbetanc4@eafit.edu.co](mailto:gbetanc4@eafit.edu.co)

Adress: Carrera 49 N° 7 Sur 50 of. 14-203, Medellín (Colombia – South America)

Phone number: (57) (4) - 261 95 00 ext. 9896

Leonel Francisco Castañeda Heredia<sup>a\*</sup>

E.mail: [lcasta@eafit.edu.co](mailto:lcasta@eafit.edu.co)

Adress: Carrera 49 N° 7 Sur 50 of. 3-313, Medellín (Colombia – South America)

Phone number: (57) (4) - 261 95 00 ext. 9368

---

\* Corresponding author. Email: [lcasta@eafit.edu.co](mailto:lcasta@eafit.edu.co)

## Identification of the state of suspension elements in railway systems

The running safety and passenger comfort levels in a vehicle are tightly related to the technical state of the suspension elements. The technical state of the suspension depends of the service life time as its components become old and wear out. A study on the dynamic behavior of a railway vehicle is established in relation to the damping elements in one of its suspension stages. An experimental measurement model is developed, obtaining a set of useful signals for the identification of the dynamic parameters of the vehicle and developing a test through the application of the OMA technique, using LSCE method as a basis to validate the numeric model of the multi-body system. Then, the study focuses on developing numeric simulations for the identification of the technical state of the dampers by the registration of dynamic variables under commercial service conditions and on estimating the state of the suspension elements.

Keywords: IRF, LSCE, multi-body model, OMA, railway testing, stabilization diagram.

### 1. Introduction

The modal properties of a dynamic system are traditionally obtained using techniques known as Experimental Modal Analysis (EMA). EMA techniques have been widely documented [1–3], nonetheless, for many cases relative to civil and mechanical structures it is difficult to apply the excitation with an impact hammer, shaker, etc. due to the size, shape, fragility or location [4].

For systems with auto-motion (aircraft, automobile, ship, train, etc.) it is necessary to know the modal parameters under normal running conditions, considering the particular characteristics of: boulder condition, distribution of forces in the frequency domain and level of response [5]; these systems possess normal operating condition which are difficult to reproduce in a laboratory, for which it is necessary to measure the physical and modal parameters during the operation.

The Operational Modal Analysis technique (OMA) is only based on the measurement of the response signals and uses the environmental excitations as non-measured signals [6]. OMA is used for the modal identification with high precision

1  
2  
3 under typical operating conditions [7]. The following are some of OMA main  
4 advantages:  
5  
6

- 7  
8  
9 • It is possible to submit to this test systems whose excitation through the  
10 application of artificial external forces do not allow to obtain correct  
11 measurements; there are mechanic systems (e.g. freight train, suburban train,  
12 tramway) for which the sources of excitation (creepage phenomenon in the  
13 contact patch on the wheel-rail interface) can not be measured individually in  
14 a precise way, and as a result an erroneous modal model is obtained [8]. The  
15 only parameters that can be measured in an exact way are the response data  
16 [9].  
17  
18
- 19 • In situ tests can be developed without interruption and in parallel with other  
20 applications. It is not necessary to move the system to a laboratory to realize  
21 the tests under controlled conditions. In situ tests avoid the need of having an  
22 express test bank [10]. In consequence, it avoids the system to be submitted to  
23 inactive time.  
24  
25
- 26 • It is a simple test procedure similar to the Operating Deflection Shapes (ODS)  
27 technique, which employs a reference transducer and various mobile response  
28 transducers. OMA does not use reference transducers in the case where all the  
29 responses are measured synchronously; on the other case, one or some  
30 transducers are used depending on the number of repeated roots that are  
31 obtained. Any of the measurements can be employed as reference, which  
32 means that OMA is a Multiple-Input Multiple-Output (MIMO) technique and  
33 allows to estimate very proximal modes with high precision [8, 10].  
34  
35  
36  
37  
38  
39  
40  
41  
42  
43  
44  
45  
46  
47  
48  
49  
50  
51  
52  
53  
54  
55  
56  
57  
58  
59  
60

1  
2  
3 A technique (see Figure 1(a)) has been adopted for the evaluation of the  
4 technical state of the dampers through the measurement of variables under operating  
5 conditions of the vehicle using the OMA-LSCE method, this meaning with the  
6 excitations of the operating conditions which originate from uncontrolled sources.  
7  
8 The present work exposes the steps to be followed in order to identify the technical  
9 state of the suspension elements.  
10  
11  
12  
13  
14  
15  
16  
17

18 Using the properties upon which the natural excitation technique [11] is based,  
19 the response functions of random noise can be used to determine the Impulse  
20 Response Function (IRF). The modal parameters of the system can be identified using  
21 standard identification methods in time domain [10]. In this paper the Least-Squares  
22 Complex Exponential method (LSCE) will be used.  
23  
24  
25  
26  
27  
28  
29  
30

31 LSCE is an OMA method in time domain whose procedure is illustrated in  
32 Figure 1(b). LSCE method determines the relation between the IRF in a Multiple  
33 Degrees of Freedom (MDoF) system, its complex poles and residues through a  
34 complex exponential. The IRF can be derived from the inverse Fourier transform (FT)  
35 for a Frequency Response Function (FRF) through the Random Decrement process  
36 (RD), or other methods. An Auto-Regressive model (AR) is constructed by the  
37 relation between poles and residues; the AR model solution allows to define a  
38 polynomial in whose roots are the complex roots of the system. Having established  
39 the roots (equivalent to the natural frequencies  $\Omega$  and the damping rates  $\xi$ ), the  
40 residues can be derived through the AR model and then obtain the modal shapes  $\phi$   
41  
42  
43  
44  
45  
46  
47  
48  
49  
50  
51  
52  
53  
54  
55  
56 [2].  
57  
58  
59  
60

The inverse Laplace transform of the transfer function of a MDoF system is the IRF,  $h_k$ . This gives as a result a series of equally spaced time intervals  $k\Delta$  ( $k = 0, 1, \dots, 2N$ ), then it is possible to express IRF as

$$h_{ij}^k = \sum_{r=1}^{2N} \phi_{ij}^{(r)} z_r^k, \quad z_r^k = e^{s_r k \Delta},$$

where

$$\phi_{ij}^{(r)} = \phi_{ij}^r = \phi_{ij}^r.$$

This expression is the product of the  $i$ th and  $j$ th elements in the modal shape  $r$ th  $\phi_r$ , and is named as the *modal constant*. The values in the series belong to the real numbers even if the residues and the roots  $s_r$  are complex values. It is possible to demonstrate that all imaginary parts will cancel each other because of the complex conjugates for both expressions:  $\phi_{ij}^{(r)}$  and  $s_r$ . The next step is to estimate the roots and the residues for the sampled data. This solution is aided by the conjugacy of the roots  $s_r$ , therefore  $z_r$ . Mathematically, this means that  $z_r$  are the roots of a polynomial with only real coefficients [4]

$$\beta_0 + \beta_1 z_r + \beta_2 z_r^2 + \dots + \beta_{2N-1} z_r^{2N-1} + \beta_{2N} z_r^{2N} = 0,$$

or

$$\sum_{k=0}^{2N} \beta_k z_r^k = 0 \iff [\beta_0 \ \beta_1 \ \beta_2 \ \dots \ \beta_{2N}]^T = \sum_{k=0}^{2N} \phi_{ij}^{(r)} z_r^k = 0 \iff \sum_{k=0}^{2N} \phi_{ij}^{(r)} z_r^k = 0$$

This equation is known as the Prony equation. The coefficients can be estimated by the IRF values.

With the calculation of the system poles, it is possible to build the stabilization diagram, which allows to graphically represent the poles of a system when it is excited in one point (reference) and measurements are made in another one (responses) [12]. The poles are codified with alphanumeric characters: stable pole (s), vibration frequency and modal vector are stable (v), vibration frequency and stifling are stable (d), only stable the vibration frequency (f), and unstable pole (o). Once the poles have been selected it is possible to estimate the vibration shapes [13].

1  
2  
3 {Figure 1}  
4  
5

## 6 **2. Description of the object of study**

7

8 The study is applied to passengers' vehicles belonging to the massive transport  
9 railway vehicle fleet of Medellin city (Colombia), which is a railway system similar to  
10 suburban trains. Original equipment manufacturer of rolling stock was MAN for  
11 mechanical components and Siemens for electrical components. MAN has since  
12 become Adtranz company and subsequently Bombardier Transportation. The vehicles  
13 are similar in geometry and design to the ET420 train sets formerly operated by  
14 Deutsche Bahn in commuter service (e.g. the Munich S-Bahn) [4, 14].  
15  
16  
17  
18  
19  
20  
21  
22  
23  
24  
25

26 The railway system has 42 three-unit cars (see Figure 2(a)). Each car has two  
27 (2) bogies that are supported over two (2) axle-wheel sets. Each car has a suspension  
28 of two (2) stages: primary and secondary [14, 15].  
29  
30  
31  
32  
33

34 The primary suspension stage is composed by elastic and damping elements  
35 that connect the axle-wheel to the bogie (helicoidal springs, guide leafs and vertical  
36 dampers); the secondary suspension stage connects the bogie to the carbody  
37 (pneumatic spring, traction link, vertical and transversal dampers).  
38  
39  
40  
41  
42  
43

44 The end cars are powered, while the center unit is an unpowered trailer car.  
45 The end cars bogies have a DC motor located in transversal position, partially  
46 suspended over the axle and over an elastic suspension connected to the bogie frame,  
47 there is one 205 kW motor per axle [14, 16].  
48  
49  
50  
51  
52  
53

54 An EMA technique [4] has been used to determine de behavior of the vehicle  
55 under a given operating condition. EMA technique is applied to a set of tests based on  
56 the excitation and the response measurement of the vehicle, according to the theory on  
57  
58  
59  
60



1  
2  
3 the classic modal analysis. The excitation of the vehicle is achieved by a manual  
4  
5 inputs applied directly to the carbody, in the location and direction necessary to  
6  
7 induce a specific shape mode. In order to be able to generate the excitation it is  
8  
9 necessary to remove the damping elements of the vehicle suspension, condition  
10  
11 denominated  $\epsilon_0$  that allows the carbody to be excited by hand.  
12  
13  
14

15  
16 To obtain a better capture of the signals in the transducers (accelerometers)  
17  
18 [17], these have been located at the ends of the carbody, collinear to the longitudinal  
19  
20 plane of the carbody. The data is realized with a minimum sample frequency of 50Hz  
21  
22 [13].  
23  
24  
25

26  
27 The set of recorded signals is transformed to the frequency domain through  
28  
29 FFT algorithm to obtain the characteristic frequencies of the carbody, finding the  
30  
31 corresponding modal shape [4, 18, 19]. Table 1 shows the results obtained from EMA  
32  
33 technique.  
34  
35  
36

37  
38 This work focuses on the study of the vehicle dynamic response [11], which is  
39  
40 influenced by the technical state of the four (4) identical vertical dampers that each  
41  
42 car has,  $\delta_j$  with  $j = 1, \dots, 4$  (see Figure 2 (b)). This type of component is characterized  
43  
44 by a set of physical laboratory tests. The test's method requires the application of  
45  
46 cyclical displacement excitation (sinusoidal) in determined ranges of frequency and  
47  
48 peak-to-peak amplitudes [4, 15, 19]. The relation obtained from the characterization  
49  
50 of the element is denominated *nominal damping function*,  $\epsilon_{10}$ . From  $\epsilon_{10}$ , a set of nine  
51  
52 (9) hypothetical properties are established,  $\epsilon_i$  with  $i = 1, \dots, 9$ . The hypothetical  
53  
54 properties have a similar behavior to  $\epsilon_{10}$ , but affected by a coefficient that reduces de  
55  
56 damping property of the element  $\delta_j$ ,  $\epsilon_i = \frac{i}{10} \epsilon_{10}$ . This is how the different technical  
57  
58  
59  
60

1  
2  
3 states of the component are represented, causing a progressive degradation of the  
4  
5 *damping function*. (Figure 2(c)).  
6  
7

8  
9 {Figure 2}

10  
11 {Table 1}

12  
13 Three (3) hypotheses are established in relation to the state of the suspension  
14  
15 elements  $\delta_j$ , which is defined parametrically by the progressive degradation of the  
16  
17 *damping function*:  
18  
19

- 20  
21  
22
- 23 • Hypothesis  $\zeta_1$ : consists on the reduction of the damping function, varying the  
24 technical state  $\epsilon_i$  of the four (4) secondary vertical hydraulic dampers  $\delta_j$ , with  
25  
26  $j = 1, \dots, 4$ .  
27  
28
  - 29 • Hypothesis  $\zeta_2$ : consists on the reduction of the damping function by varying  
30 the technical state  $\epsilon_i$  of the two (2) leading dampers ( $\delta_1, \delta_2$ ), these being the  
31  
32 ones located at the closest distance to the driver; the other two (2) dampers ( $\delta_3,$   
33  
34  $\delta_4$ ) conserve the nominal property  $\epsilon_{10}$ .  
35  
36  
37
  - 38 • Hypothesis  $\zeta_3$ : consist on the reduction of the damping function by varying the  
39 technical state  $\epsilon_i$  of the two (2) training dampers, these being the ones located  
40  
41 at the end opposite to the driver ( $\delta_3, \delta_4$ ); the other two (2) dampers ( $\delta_1, \delta_2$ )  
42  
43 conserve the nominal property  $\epsilon_{10}$ .  
44  
45  
46  
47  
48  
49  
50

### 51 52 53 **3. Development of numeric models**

54  
55 A model of the railway vehicle can be developed and put in motion on a typical track  
56  
57 and instrumented in a virtual environment, which allows investigating the effects of a  
58  
59 wide range of possible variations of the vehicle parameters [4, 11]. The results  
60

1  
2  
3 obtained from a model can provide accurate predictions of the dynamic behavior of  
4  
5 the vehicle and the interaction with the track [20 – 22].  
6  
7

8  
9 The general approach of a virtual model is to numerically integrate the  
10  
11 ordinary differential equation that constitutes the model by using one or various  
12  
13 integration algorithms. This approach is usually denominated simulation or numerical  
14  
15 experimentation, which is equivalent to physical experimentation where the system is  
16  
17 subject to given conditions and its response is registered. This approach is convenient  
18  
19 because it [3]:  
20  
21  
22

- 23 • allows to different types of models and complexity degree; and
- 24 • evaluating the response of any type of perturbation.  
25  
26  
27  
28  
29

30  
31 But it has limitations such as [3]:  
32  
33

- 34 • does not allow identifying the whole behavior of the system, only the response  
35 under defined conditions;  
36  
37
- 38 • requires computing resources. It generates high computational costs in cases  
39 where the system is complex or the model has characteristics that make the  
40  
41 numeric integration a difficult procedure; and  
42  
43
- 44 • allows the variation effects of the parameters to be predicted, only with a high  
45  
46 quantity of simulations.  
47  
48  
49  
50

51  
52 The numeric model used to simulate the characteristics of the system is  
53  
54 considered to be a true virtual prototype. The virtual techniques allow the model to  
55  
56 generate information on the dynamic behavior and the interaction of the components,  
57  
58 which are only comparable to physical prototypes. Simulations with numeric models  
59  
60 are a valid source of the necessary data to apply the formulated methodology. The

1  
2  
3 virtual techniques allow the model to generate a great quantity of information not only  
4  
5 on response and dynamic behavior, but also relative to the interaction of the  
6  
7 components, load details and even aesthetic qualities that are only comparable to  
8  
9 physical prototypes [4, 11, 12, 21].  
10  
11

12  
13  
14 The numeric model developed has 120 DoF [15], the model consist of the  
15  
16 union of two (2) simplified models (see Figure 3(a)) and represents a complete motor  
17  
18 car (see Figure 3(b)). It is based on the multi-body system theory, using the analysis  
19  
20 software VAMPIRE® [23]; the values of the particular parameters of the model are  
21  
22 exposed in Appendix 2.  
23  
24

25  
26  
27 {Figure 3}  
28

#### 29 **4. Test development in a virtual environment**

30  
31 It is necessary to point out the guidelines for the correct development of the test. The  
32  
33 coherent design of the experiment allows a correct analysis of the data and it must be  
34  
35 designed to evaluate the secondary suspension under normal operating and controlled  
36  
37 conditions, without affecting the operation and the security of the system. The test is  
38  
39 defined following these conditions:  
40  
41  
42

- 43  
44 • the necessary load condition (AW0), this meaning that the car is empty;
- 45  
46 • the section track is straight track and the track irregularities are considered  
47  
48 [24];  
49
- 50  
51 • the vehicle speed,  $V=80\text{km/h}$ ; and
- 52  
53 • a variation of the secondary suspension dampers technical state is assumed  $\epsilon i$   
54  
55 (see Figure 2 (c)).  
56  
57  
58  
59  
60

The measurement points are defined according to the railway international standards [25]. Given that the interest of this work focuses on the study of the secondary stage vertical suspension, the signals to be recorded must in the main bodies of the system, in this way three (3) signals in vertical direction are chosen. The signals are located in:

- $\bar{z}_{q1}^+$ , on the floor of the carbody, at leader side (**Error! Reference source not found.**(a));
- $\bar{z}_{q1}^+$ , in the bogie frame near to the attack axle (Figure 4(b)); and
- $\bar{z}_{q1}^0$ , in the axlebox of the attack axle (**Error! Reference source not found.**(c)).

{Figure 4}

## 5. Processing and results with the OMA-LSCE method

The set of signals  $\bar{z}_{q1}^+$ ,  $\bar{z}_{q1}^+$ , and  $\bar{z}_{q1}^0$  is processed by the OMA-LSCE method, based on the measurement of response of the system to the excitations of the operation and from which the global modal parameters are estimated:  $\Omega$ ,  $\xi$  and  $\phi$  [12]. The modal parameters are graphically represented by the stabilization diagrams. Appendix 3 exposes as an example a set of stabilization diagrams obtained from different operating conditions of the vehicle. In the diagrams it is possible to identify:

- two (2) local maximums in the range [1, 2.5]Hz, which correspond to the two (2) modal shapes (bounce  $\phi_2$ , and pitch  $\phi_4$ ) and are registered in the carbody by the sensor  $\bar{z}_{q1}^+$  ;

- three (3) local maximums in the range [4, 10]Hz, which correspond to the three (3) modal shapes recorded from the bogie by the sensor  $\dot{z}_{q1}^+$ ; and
- three (3) local maximums in the range [15, 25]Hz, which correspond to the vertical irregularities of the track and are obtained from the signal registered by sensor  $\dot{z}_{q1}^o$ .

The work focuses on the analysis of the vehicle, more specifically in the carbody for which it has been possible to identify two (2) vertical modal shapes ( $\phi_2$ ,  $\phi_4$ ) under the load condition AW0, see Table 2.

{Table 2}

## 6. Analysis of the results

From the set of values of the modal parameters identified for the different hypothesis  $\zeta_i$  it is possible to show the existing relationship between the technical state of the damping set and:

- the natural frequency  $\Omega$ , of the modal shape  $\phi_2$  y  $\phi_4$ , obtaining regressive lineal models with a correlation coefficient value of  $\sqrt{R^2} > 0.98$  (see Figure 5); and
- the damping rate  $\xi$ , obtaining regressive exponential models with correlation coefficient values of  $\sqrt{R^2} > 0.96$  (see Figure 6).

The regressive models are considered valid given that the values  $\sqrt{R^2}$  represent an association measurement of the statistical model with the obtained data [26], which have an acceptable level for the reach of this work.

{Figure 5}

{Figure 6}

## 7. Validation of the test

The regressive models belonging to  $\zeta_1$  and obtained by OMA-LSCE in a virtual environment are extrapolated to the value of the technical state of the damper with a null *damping function*,  $\epsilon_0$ , for the modal shapes  $\phi_i$ , meaning:

$$\begin{aligned} &\text{for } \phi_2, \\ \epsilon(\omega) &= 9.577 \left( \omega - 13.950 \right) \cdot \omega \quad \text{if } \omega \in [\epsilon_0, \omega_0] \rightarrow \omega_0 = 1.46 \text{Hz} \quad , \text{ and} \\ &\text{for } \phi_4, \epsilon(\omega) = 8.761 \left( \omega - 18.326 \right) \cdot \omega \quad \text{if } \omega = \epsilon_0 \rightarrow \omega = 2.09 \text{Hz} \quad . \end{aligned}$$

In this way the dynamic behavior of the vehicle without the secondary damper is obtained, emulating the whole extraction of the damping elements of the suspension  $\delta_j$  with  $j = 1, \dots, 4$ ; which is the same testing condition realized to the vehicle with the EMA technique.

The values reordered by the two (2) types of analysis, EMA and OMA, are compared (see Table 2) which allows observing that there is an estimation error of the modal parameter,  $(\% < 1\%)$ . Therefore, it is possible to consider valid the regressive models given that the  $\epsilon$  values represent an acceptable deviation level for the reach of this work.

{Table 3}

## 8. Case study, application of the regressive models

Given the set of signals,  $\bar{z}_{q1}^+$ ,  $\bar{z}_{q1}^-$ , y  $\bar{z}_{q1}^0$ , obtained from a car. The data has been processed through OMA-LSCE, the following identification of modal parameters is obtained:

- natural frequency:  $\Omega = 1.53$  Hz for  $\phi_2$ , and  $\Omega = 2.18$  Hz for  $\phi_4$ ; and
- damping rate:  $\xi = 2.90$  % for  $\phi_2$ , and  $\xi = 2.20$  % for  $\phi_4$ .

Starting from the identified modal parameters and based on the series of regressive models obtained for the vehicle, the probable state of the damper is identified  $\epsilon_i$ , for each one of the hypothesis  $\zeta_i$ . The regressive models in the identification of the modal shape  $\phi_2$  are:

$$\begin{aligned} \text{for } \zeta_1, \epsilon(\Omega) &= 9.577 \left( - 13.950 \right) \therefore \epsilon(1.53) = 0.70, \\ \epsilon(\xi) &= 0.084e^{0.733\xi} \quad \therefore \epsilon(2.90) = 0.70, \\ \text{for } \zeta_2, \epsilon(\Omega) &= 13.161 \left( - 19.567 \right) \therefore \epsilon(1.53) = 0.57, \\ \epsilon(\xi) &= 0.027e^{1.056\xi} \quad \therefore \epsilon(2.90) = 0.58, \\ \text{for } \zeta_3, \epsilon(\Omega) &= 13.958 \left( - 20.873 \right) \therefore \epsilon(1.53) = 0.48; \\ \epsilon(\xi) &= 0.008e^{1.365\xi} \quad \therefore \epsilon(2.90) = 0.42; \end{aligned}$$

in the modal shape  $\phi_4$  are:

$$\begin{aligned} \text{for } \zeta_1, \epsilon(\Omega) &= 8.761 \left( - 18.326 \right) \therefore \epsilon(2.18) = 0.77, \\ \epsilon(\xi) &= 7.207E-5e^{4.151\xi} \quad \therefore \epsilon(2.20) = 0.67, \\ \text{for } \zeta_2, \epsilon(\Omega) &= 23.326 \left( - 50.240 \right) \therefore \epsilon(2.18) = 0.61, \\ \epsilon(\xi) &= 1.855E-4e^{3.773\xi} \quad \therefore \epsilon(2.20) = 0.75, \\ \text{for } \zeta_3, \epsilon(\Omega) &= 25.431 \left( - 54.825 \right) \therefore \epsilon(2.18) = 0.61; \\ \epsilon(\xi) &= 5.334E-4e^{3.279\xi} \quad \therefore \epsilon(2.20) = 0.72. \end{aligned}$$

The  $\epsilon$  values from the hypothesis  $\zeta_i$  are tabulated (Table 4). The mean of the technical state is calculated,  $\bar{X}_i$  as well as their corresponding standard deviation  $\sigma_i$ , the later will be the criteria that defines the valid hypothesis  $\zeta_i$ . The  $\zeta_i$  that presents the least standard deviation is the one that adapts to the obtained dynamic characteristics of the system and therefore the value  $\bar{X}_i$  of such hypothesis must be the technical state of the damper  $\epsilon$ , meaning  $\zeta_i = \bar{X}_i(\epsilon) \nabla \min(\sigma_i)$ .



The technical state of the damper is  $\epsilon = \bar{X}(\epsilon) \mp 2\sigma$  with 95.45% of confidence factor. For the given case study, the value of the technical state is  $\epsilon = 0.71\epsilon_{10} \pm 0.1$  in the four (4) secondary stage vertical dampers (hypothesis  $\zeta_1$ ) with a confidence of 95.45%. This means that the dampers are degraded 29% relative its nominal characteristic.

{Table 4}

## 9. Conclusions

The OMA-LSCE technique is a suitable technique to evaluate and identify the technical state of the dampers  $\epsilon_i$  and the operating characteristics of the components of passengers railway vehicles.

The vertical dampers of the secondary suspension stage present a direct influence on the dynamic behavior of the modal shapes,  $\phi_2$  and  $\phi_4$ , therefore the different technical states of the damper  $\epsilon_i$  can be tested and estimated through the dynamic recording in the carbody. This means that from the sensors installed in the carbody that register appropriately the natural frequency  $\Omega$  it is possible to determine the variation of the damping function of these elements and to infer their degradation or failure.

The dynamic parameters,  $\Omega$  and  $\xi$ , have a high dependence degree over the secondary suspension dampers  $\delta_j$ .

An experimental model of three (3) measurement points,  $\dot{z}_{qt}^*$ ,  $\dot{z}_{qt}^+$ , y  $\dot{z}_{qt}^o$  obtained from a set of sensors can be used to identify the dynamic parameters,  $\Omega$  and  $\xi$ , in a vehicle with load condition AW0 with the OMA-LSCE method.

A methodology has been proposed and applied for the evaluation of the technical state of the dampers  $\epsilon_i$  and the identification of hypothesis of suspension elements deterioration  $\zeta_i$  through measurements of variables under operating conditions of the vehicle.

International standards for railway vehicles define the range for deficient frequency  $\omega = [8,10]\text{Hz}$ . The human body is sensible to vertical accelerations [27]; frequencies  $\omega \approx 10\text{Hz}$  cause excessive oscillations on  $\phi_2$ , generating significant deficiency of comfort. Comparing with the values obtained for the analyzed vibration modes  $\phi_r$  and under the different technical states of the damper  $\epsilon_i$ , the natural frequency is  $\Omega < 2\text{Hz}$ . Therefore, the degradation of the damping function of the suspension elements does not incur *per se* in violation to the railway standard.

### Appendix 1. Notation

#### *Abbreviations, acronyms, coefficients and constants*

AR	Auto-regression model.
AW0	<i>Anhängerladung Wägestück 0</i> (load weight 0; empty car).
DC	Direct Current.
DoF	Degrees of Freedom.
EMA	Experimental Modal Analysis.
FFT	Fast Fourier Transform.
FRF	Frequency Response Function.
FT	Fourier Transform.
IRF	Impulse Response Function.
LSCE	Least-Squares Complex Exponential.
MAN	<i>Maschinenfabrik Augsburg-Nürnberg.</i>
MDoF	Multiple Degrees of Freedom.
MIMO	Multiple Input Multiple Output.
ODS	Operating Deflection Shapes.
OMA	Operational Modal Analysis.
FT	Fourier Transform.
RD	Random Decrement process.
$(\alpha_r)^{-1} A^{-1} \Gamma_{ij}$	$r$ th modal constant.
$h_k$	$k$ th IRF.
$k\Delta$	Time interval.
$R^2$	Coefficient of determination.

$\sqrt{R^2}$	Coefficient of correlation.
$s_r$	$r$ th complex quantity root.
$\bar{X}_i \quad i = 1, 2, 3$	$i$ th mean
$V$	Vehicle speed.
$z_r$	Conjugacy of the roots $s_r$ .
$\ddot{z}_{q1}^c, \ddot{z}_{q1}^l, \ddot{z}_{q1}^a$	Vertical acceleration at carbody, leader bogie and attack axlebox, respectively.
$\Omega$	Natural frequency.
$\alpha(\omega)$	Receptance matrix
$\beta_k \quad k = 0, 1, \dots, 2$	$k$ th real coefficient.
$\delta_j \quad j = 1, \dots, 4$	$j$ th secondary vertical damper.
$\varepsilon$	Error value.
$\epsilon_i \quad i = 1, \dots, 10$	$i$ th damper technical state.
$\phi_r$	$r$ th mode shape.
$\sigma_i \quad i = 1, 2, 3$	$i$ th standard deviation
$\Omega$	Oscillation frequency.
$\xi$	Damping rate.
$\zeta_i \quad i = 1, 2, 3$	$i$ th hypothesis

## Appendix 2. Vehicle parameters

{Table 5}

## Appendix 3. Stabilization diagrams

{Figure 7}

## References

- [1] D.J. Ewins, *Modal Testing: Theory, Practice and Application*, Mechanical Engineering Research Studies Engineering Dynamics Series, Research Studies Press, Second Ed, Hertfordshire, UK, 2000
- [2] J. He, and Z.F. Fu, *Modal Analysis*, Butterworth-Heinemann, UK, 2001.
- [3] G. Genta, *Vibration Dynamics and Control*, Springer Science Business, Torino, Italy, 2009.
- [4] L.F. Castañeda, and B. Żółtowski, *Estudio de Explotación de vehículos Ferroviarios*, Fondo Editorial Universidad EAFIT, Colombia, 2009.
- [5] T. Nagayama, M. Abe, Y. Fujino, and K. Ikeda, Structural Identification of a Nonproportionally Damped System and its Application to a Full-Scale Suspension Bridge, *Int J. Struct. Eng.* 131(2005) pp. 1536-1545.
- [6] N.J. Jacobsen, and O. Thorhauge, *Data Acquisition Systems for Operational Modal Analysis*, IOMAC – 3<sup>rd</sup> Int. Operational Modal Analysis Conf., Nærum, Denmark, 2009.
- [7] N.B. Møller, H. Herlufsen, and S. Gade, *Modal Parameters from a Wind Turbine Wing by Operational Modal Analysis*, 32<sup>nd</sup> International Congress and Exposition on Noise Control Engineering, Seogwipo, Korea, 2003.

- 1  
2  
3  
4 [8] E. Yousaf, *Output Only Modal Analysis*, MSc thesis, Mechanical Engineering  
5 Department, Blekinge Institute of Technology, Karlskrona, Sweden, 2007.
- 6 [9] N.J. Jacobsen, P. Andersen, and R. Brincker, *Using Enhanced Frequency Domain*  
7 *Decomposition as a Robust Technique to Harmonic Excitation in Operational*  
8 *Modal Analysis*, ISMA - Int. Conf. on Noise and Vibration Engineering,  
9 Leuven, Belgium. 2006.
- 10 [10] T. Uhl, and P. Kurowski, *Vioma User's Guide*, University of Mining and  
11 Metallurgy in Kraków Press, Poland, 2002.
- 12 [11] K. Goda and R Goodall, Fault-Detection-and-Isolation System for a Railway  
13 Vehicle Bogie, in *The Dynamics of Vehicles on Roads and on Tracks*, M. Abe,  
14 ed., Taylor & Francis, Vol. 41, UK, 2003, pp. 468-476.
- 15 [12] T. Uhl, *The Inverse Identification Problem and its Technical Application*,  
16 Springer-Verlag, 2006.
- 17 [13] GEMI Research Group, *Análisis Modal en Vehículos Ferroviarios Sistema de*  
18 *Transporte Metro de Medellín* - , Final Tech. Rep. Mechanical Project  
19 Research, EAFIT University, Colombia, 2010.
- 20 [14] M.E. Palacio, *Implementación de la Norma UIC518 en Vehículos de Pasajeros*  
21 *para el Metro de Medellín, con Énfasis en el Análisis de Ruido Emitido por*  
22 *los Vehículos*, M.Sc. thesis, Mechanical Engineering Department, EAFIT  
23 University, Colombia, 2006.
- 24 [15] R.M. Martinod, L.F. Castañeda, J.A. Gallego, *Dynamic Analysis to Evaluate*  
25 *Stability, Safety and Confort in Railway Vehicles*, ISPE - 23<sup>rd</sup> Int. Conf. on  
26 CAD/CAM Robotics and Factories of the Future, Colombia, 2007, pp.403-  
27 408.
- 28 [16] UTB, *Mediciones Experimentales de Esfuerzos Dinámicos en Marcha. Metro de*  
29 *Medellín*, Tech. Rep. Universität Technshe Berlin, Colombia. 1997.
- 30 [17] J. Stow, and E. Andersson, *Field testing and Instrumentation of Railway*  
31 *Vehicles*, in in *Handbook of Railway Vehicle Dynamics*, S. Iwnicki, ed.,  
32 Taylor & Francis, USA, 2006.
- 33 [18] C.W. De Silva, *Vibration, Fundamentals and Practice*, Taylor & Francis, Second  
34 Ed, USA, 2007.
- 35 [19] GEMI Research Group, *Damper Parameters Analysis of Metro de Medellín*,  
36 Final Tech. Rep. PV01, Mechanical Project Research, EAFIT University,  
37 Colombia, 2009.
- 38 [20] R.M. Goodall, and S. Iwnicki, *Non-Linear Dynamic techniques v. Equivalent*  
39 *Conicity Methods for Rail Vehicle Stability Assessment*, in *The Dynamics of*  
40 *Vehicles on Roads and on Tracks*, M. Abe, ed., Taylor & Francis, Vol. 41,  
41 UK, 2003, pp. 791-799.
- 42 [21] O. Polach, M. Berg, and S Iwnicki, *Simulation*, in , in *Handbook of Railway*  
43 *Vehicle Dynamics*, S. Iwnicki, ed., Taylor & Francis, USA, 2006.
- 44 [22] A.H. Wickens, *Fundamentals of Rail Vehicle Dynamics. Guidance and Stability*,  
45 Swets & Zeitlinger, USA, 2003.
- 46 [23] A.J. Minnis, *Vampire Product Quality & Certification*, DeltaRail Group Limited,  
47 UK, 2007.
- 48 [24] K. Knothe, *Benchmark Test for Models of Railway Track Ans of Vehicle/Track*  
49 *Interaction in Low Frequency Range*, in *Iteration of Railway Vehicles whith*  
50 *Track and its Substructure*, K. Knothe, S. Grassie, and J. Elkins, eds., Swets &  
51 Zeitlinger, Vol. 24, 1995, pp. 363-379.
- 52  
53  
54  
55  
56  
57  
58  
59  
60

- 1  
2  
3 [25] UIC 518, *Testing and Approval of Railway Vehicle from the Point of View of*  
4 *Their Dynamic Behaviour – Safety – Track Fatigue – Ride Quality*,  
5 International Union of Railways, Third Ed, France, 2005.  
6  
7 [26] E.L. Grant, *Statistical Quality Control*, McGraw Hill, Third Ed, USA, 1964.  
8  
9 [27] ISO 2631-1, *Mechanical Vibration and Shock – Evaluations of Human Exposure*  
10 *to whole Body Vibration – Part 4: Guidelines for the Evaluation of the Effects*  
11 *of Vibration and Rotational Motion on Passengers and Crew Comfort of Fixed*  
12 *Guideway Transport Systems*, International Standards Organization, Genève,  
13 Switzerland, 2001.  
14 [28] D. Thomson, and J. Jones, Noise and Vibration from Raylways Vehicles, in  
15 *Handbook of Railway Vehicle Dynamics*, S. Iwnicki, ed., Taylor & Francis,  
16 USA, 2006.  
17  
18  
19  
20  
21  
22  
23  
24  
25  
26  
27  
28  
29  
30  
31  
32  
33  
34  
35  
36  
37  
38  
39  
40  
41  
42  
43  
44  
45  
46  
47  
48  
49  
50  
51  
52  
53  
54  
55  
56  
57  
58  
59  
60

1  
2  
3  
4  
5  
6  
7  
8  
9  
10  
11  
12  
13  
14  
15  
16  
17  
18  
19  
20  
21  
22  
23  
24  
25  
26  
27  
28  
29  
30  
31  
32  
33  
34  
35  
36  
37  
38  
39  
40  
41  
42  
43  
44  
45  
46  
47  
48  
49  
50  
51  
52  
53  
54  
55  
56  
57  
58  
59  
60

Figure 1. Flowchart of the process: (a) Mathematical development; and (b) OMA-LSCE method.

Figure 2. Railway vehicle: (a) unit of three (3) cars; (b) Location of the secondary dampers; and (c) Damping function of the secondary dampers.

Figure 3: Graphic representation of the numeric models: (a) simple model; and (b) complete model.

Figure 4. Location of the sensors: (a) In the passengers' box  $\bar{z}_{q1}^+$ ; (b) On the bogie  $\bar{z}_{q1}^+$ ; and (c) In the axle box  $\bar{z}_{q1}^o$ .

Figure 5. Development of regressive models  $\zeta$ , modal parameter  $\Omega$ .

Figure 6. Development of regressive models  $\zeta$ , modal parameter  $\xi$ .

Figure 7. Estabilization diagrams: (a) Hyphotesis  $\zeta_1$  with  $\epsilon_1$ ; (b) Hyphotesis  $\zeta_1$  with  $\epsilon_9$ ; (c) Hyphotesis  $\zeta_2$  with  $\epsilon_1$ ; (d) Hyphotesis  $\zeta_2$  with  $\epsilon_9$ ; (e) Hyphotesis  $\zeta_3$  with  $\epsilon_1$ ; and (f) Hyphotesis  $\zeta_3$  with  $\epsilon_9$ .

1  
2  
3  
4  
5  
6  
7  
8  
9  
10  
11  
12  
13  
14  
15  
16  
17  
18  
19  
20  
21  
22  
23  
24  
25  
26  
27  
28  
29  
30  
31  
32  
33  
34  
35  
36  
37  
38  
39  
40  
41  
42  
43  
44  
45  
46  
47  
48  
49  
50  
51  
52  
53  
54  
55  
56  
57  
58  
59  
60

Table 1. Modal parameters identify by EMA technique, condition  $\epsilon_0$ .

Modal shape, $\phi_r$	Lower roll, $\phi_1$	Bounce, $\phi_2$	Yaw, $\phi_3$	Pitch, $\phi_4$
Natural frequency, $\Omega$ [Hz]	0.80	1.47	1.50	2.10

For Peer Review Only

Table 2. Modal parameters identified by OMA-LSCE technique.

Technical state of damper, $\epsilon_i$	$\zeta_1$		$\zeta_2$				$\zeta_3$					
	$\phi_2$	$\phi_4$	$\phi_2$	$\phi_4$	$\phi_2$	$\phi_4$	$\phi_2$	$\phi_4$				
	$\Omega$ [Hz]	$\xi$ [%]	$\Omega$ [Hz]	$\xi$ [%]	$\Omega$ [Hz]	$\xi$ [%]	$\Omega$ [Hz]	$\xi$ [%]	$\Omega$ [Hz]	$\xi$ [%]	$\Omega$ [Hz]	$\xi$ [%]
$\epsilon_1$	1.479	0.820	2.095	1.727	1.480	0.851	2.102	1.994	1.498	1.768	2.159	1.594
$\epsilon_2$	1.480	1.001	2.112	1.882	1.480	1.001	2.112	1.882	1.502	1.987	2.160	1.785
$\epsilon_3$	1.484	1.364	2.128	2.070	1.484	1.364	2.128	2.070	1.520	2.752	2.166	1.910
$\epsilon_4$	1.491	1.876	2.144	2.136	1.491	1.876	2.144	2.136	1.526	2.745	2.170	2.037
$\epsilon_5$	1.504	2.395	2.159	2.154	1.504	2.395	2.159	2.154	1.544	3.965	2.179	2.300
$\epsilon_6$	1.515	2.757	2.167	2.190	1.515	2.757	2.167	2.190	1.559	5.410	2.184	2.596
$\epsilon_7$	1.517	3.105	2.177	2.255	1.539	5.567	2.224	9.562	1.551	3.696	2.186	2.308
$\epsilon_8$	1.543	3.239	2.184	2.230	1.543	3.239	2.184	2.230	1.552	3.131	2.189	2.224
$\epsilon_9$	1.553	3.363	2.190	2.248	1.553	3.363	2.190	2.248	1.558	3.294	2.192	2.263
$\epsilon_{10}$	1.561	3.449	2.195	2.273	1.561	3.449	2.195	2.273	1.562	3.511	2.196	2.322



1  
2  
3  
4  
5  
6  
7  
8  
9  
10  
11  
12  
13  
14  
15  
16  
17  
18  
19  
20  
21  
22  
23  
24  
25  
26  
27  
28  
29  
30  
31  
32  
33  
34  
35  
36  
37  
38  
39  
40  
41  
42  
43  
44  
45  
46  
47  
48  
49  
50  
51  
52  
53  
54  
55  
56  
57  
58  
59  
60

Table 3. Modal parameters identified by EMA and OMA techniques, condition  $\epsilon_0$ .

Modal analysis type	Modal shape $\Omega$ [Hz]	
	$\phi_2$	$\phi_4$
EMA	1.47	2.10
OMA	1.46	2.09
Error, $\epsilon$ [%]	0.91	0.04

For Peer Review Only

Table 4. Evaluation of technical state  $\epsilon$  in order to  $\zeta_i$ .

Modal shape, $\phi_r$	Modal parameter		technical state of damper $\epsilon$ [--]		
	Description	Value	$\zeta_1$	$\zeta_2$	$\zeta_3$
$\phi_2$	$\Omega$ [Hz]	1.53	0.70	0.57	0.48
	$\xi$ [%]	2.90	0.70	0.58	0.42
$\phi_4$	$\Omega$ [Hz]	2.18	0.77	0.61	0.61
	$\xi$ [%]	2.20	0.67	0.75	0.72
Mean value, $\bar{x}_i$			0.71	0.63	0.56
Standard deviation, $\sigma_i$			0.04	0.08	0.14

Table 5. Vehicle parameters.

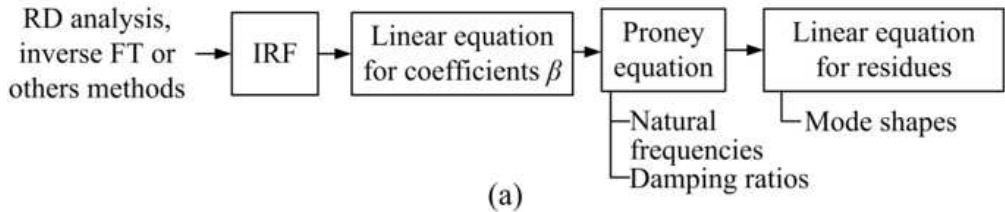
Element	Quantity	Value	Unit
Mass			
Carbody	1	24486.36	kg
Bogie frame	2	6102.44	kg
Motor	4	5551	kg
Electromag. brake	4	704	kg
Traction link	2	--	kg
Axle-wheel set	4	7083.52	kg
Stiffness			
Lineal	1	$k_A = 1.00$	kN/mm
Non-lineal	20	--	kN/mm
Shear	8	$k_x = 2.16$	kN/mm
		$k_y = 2.16$	kN/mm
		$k_z = 12.16$	kN/mm
Axi-directional	2	0.08	kNmm/s
Air stiffness	4	$k_z = 4.52$	kN/mm
		$k_y = 1.04$	kN/mm
Non-lineal damper	13	--	kNmm/s
Busing	36	$k_x = 67.32$	kN/mm
		$k_y = 36E-5$	kN/mm

1  
2  
3  
4  
5  
6  
7  
8  
9  
10  
11  
12  
13  
14  
15  
16  
17  
18  
19  
20  
21  
22  
23  
24  
25  
26  
27  
28  
29  
30  
31  
32  
33  
34  
35  
36  
37  
38  
39  
40  
41  
42  
43  
44  
45  
46  
47  
48  
49  
50  
51  
52  
53  
54  
55  
56  
57  
58  
59  
60

Element	Quantity	Value	Unit
		$k_z = 72E-6$	kN/mm
		$k_\theta = 36E-5$	MNm/rad
		$k_\phi = 2E-6$	MNm/rad
		$k_\psi = 1E-5$	MNm/rad
DOF	120	--	--
Conicity non-linear		--	--

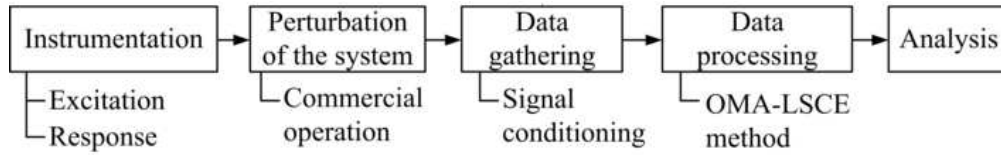
For Peer Review Only

1  
2  
3  
4  
5  
6  
7  
8  
9  
10  
11  
12  
13  
14  
15  
16  
17  
18  
19  
20  
21  
22  
23  
24  
25  
26  
27  
28  
29  
30  
31  
32  
33  
34  
35  
36  
37  
38  
39  
40  
41  
42  
43  
44  
45  
46  
47  
48  
49  
50  
51  
52  
53  
54  
55  
56  
57  
58  
59  
60



28x6mm (600 x 600 DPI)

or Peer Review Only



(b)

29x6mm (600 x 600 DPI)

or Peer Review Only

1  
2  
3  
4  
5  
6  
7  
8  
9  
10  
11  
12  
13  
14  
15  
16  
17  
18  
19  
20  
21  
22  
23  
24  
25  
26  
27  
28  
29  
30  
31  
32  
33  
34  
35  
36  
37  
38  
39  
40  
41  
42  
43  
44  
45  
46  
47  
48  
49  
50  
51  
52  
53  
54  
55  
56  
57  
58  
59  
60

1  
2  
3  
4  
5  
6  
7  
8  
9  
10  
11  
12  
13  
14  
15  
16  
17  
18  
19  
20  
21  
22  
23  
24  
25  
26  
27  
28  
29  
30  
31  
32  
33  
34  
35  
36  
37  
38  
39  
40  
41  
42  
43  
44  
45  
46  
47  
48  
49  
50  
51  
52  
53  
54  
55  
56  
57  
58  
59  
60

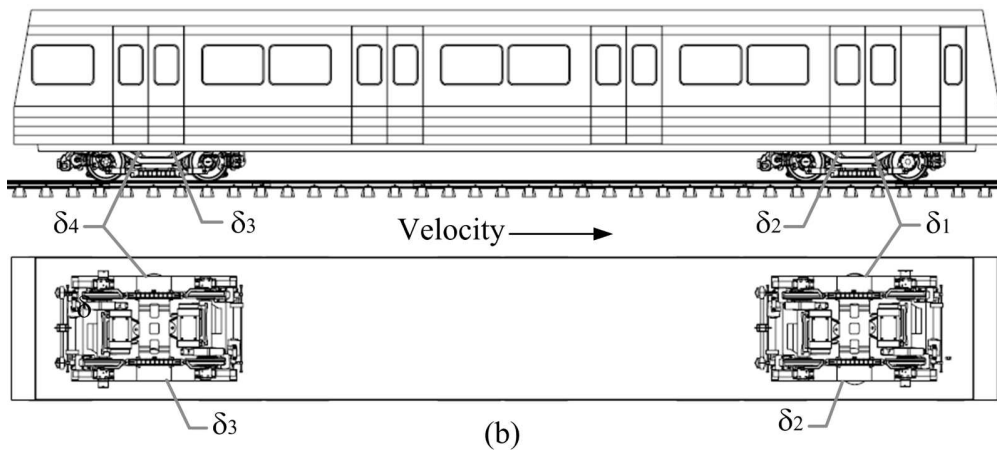


(a)

135x38mm (600 x 600 DPI)

Peer Review Only

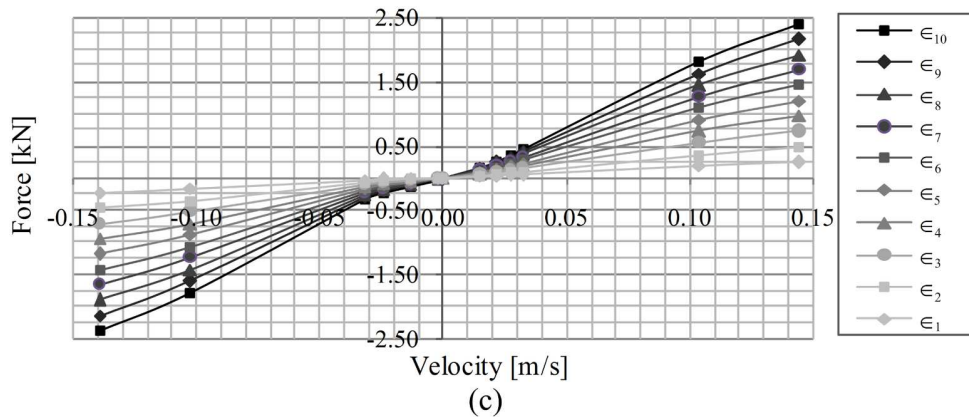
1  
2  
3  
4  
5  
6  
7  
8  
9  
10  
11  
12  
13  
14  
15  
16  
17  
18  
19  
20  
21  
22  
23  
24  
25  
26  
27  
28  
29  
30  
31  
32  
33  
34  
35  
36  
37  
38  
39  
40  
41  
42  
43  
44  
45  
46  
47  
48  
49  
50  
51  
52  
53  
54  
55  
56  
57  
58  
59  
60



135x61mm (600 x 600 DPI)

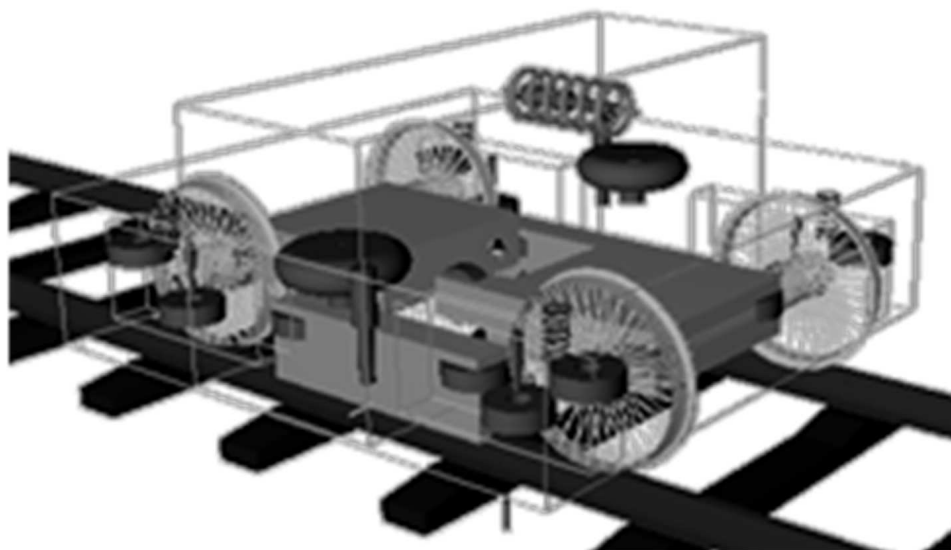


1  
2  
3  
4  
5  
6  
7  
8  
9  
10  
11  
12  
13  
14  
15  
16  
17  
18  
19  
20  
21  
22  
23  
24  
25  
26  
27  
28  
29  
30  
31  
32  
33  
34  
35  
36  
37  
38  
39  
40  
41  
42  
43  
44  
45  
46  
47  
48  
49  
50  
51  
52  
53  
54  
55  
56  
57  
58  
59  
60



135x56mm (600 x 600 DPI)

Peer Review Only



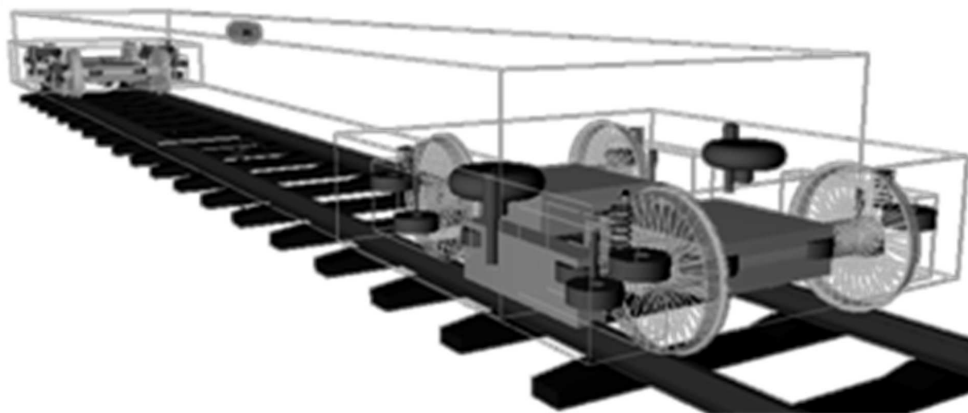
(a)

64x41mm (600 x 600 DPI)

Review Only

1  
2  
3  
4  
5  
6  
7  
8  
9  
10  
11  
12  
13  
14  
15  
16  
17  
18  
19  
20  
21  
22  
23  
24  
25  
26  
27  
28  
29  
30  
31  
32  
33  
34  
35  
36  
37  
38  
39  
40  
41  
42  
43  
44  
45  
46  
47  
48  
49  
50  
51  
52  
53  
54  
55  
56  
57  
58  
59  
60

1  
2  
3  
4  
5  
6  
7  
8  
9  
10  
11  
12  
13  
14  
15  
16  
17  
18  
19  
20  
21  
22  
23  
24  
25  
26  
27  
28  
29  
30  
31  
32  
33  
34  
35  
36  
37  
38  
39  
40  
41  
42  
43  
44  
45  
46  
47  
48  
49  
50  
51  
52  
53  
54  
55  
56  
57  
58  
59  
60

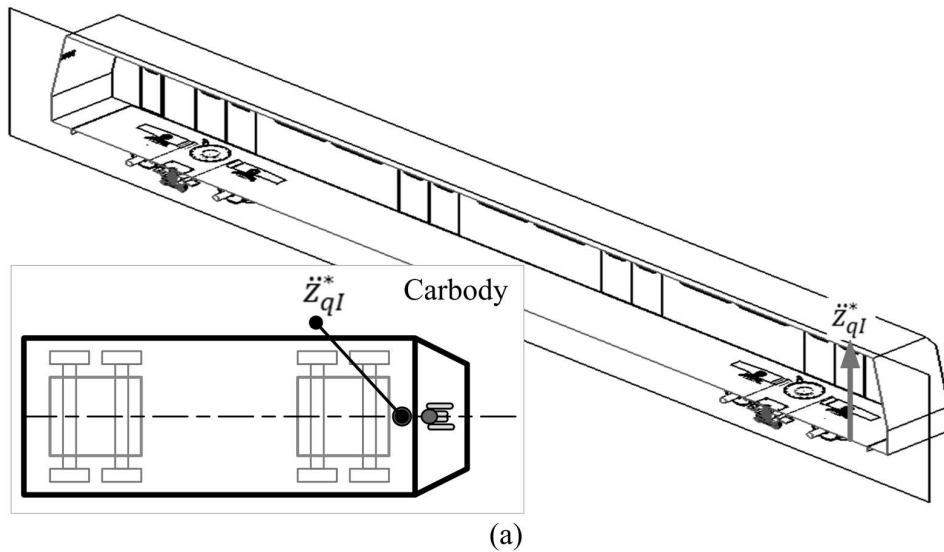


(b)

82x41mm (600 x 600 DPI)

Review Only

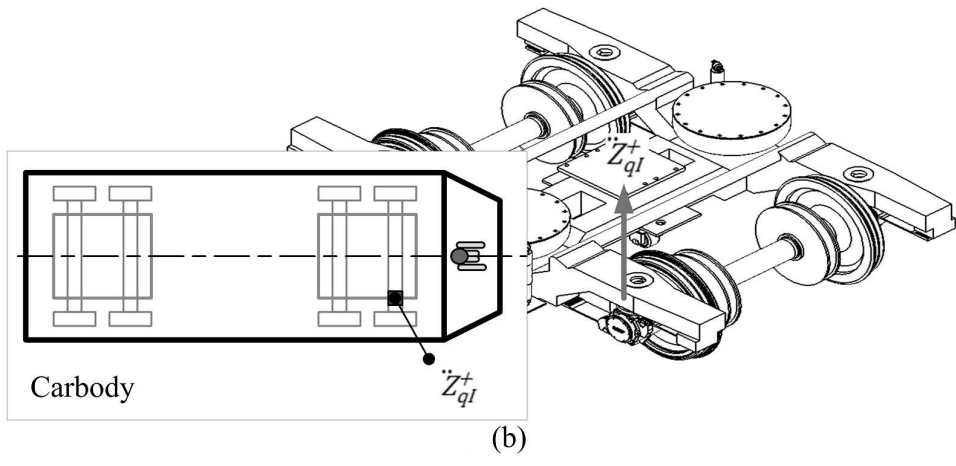
1  
2  
3  
4  
5  
6  
7  
8  
9  
10  
11  
12  
13  
14  
15  
16  
17  
18  
19  
20  
21  
22  
23  
24  
25  
26  
27  
28  
29  
30  
31  
32  
33  
34  
35  
36  
37  
38  
39  
40  
41  
42  
43  
44  
45  
46  
47  
48  
49  
50  
51  
52  
53  
54  
55  
56  
57  
58  
59  
60



139x77mm (600 x 600 DPI)

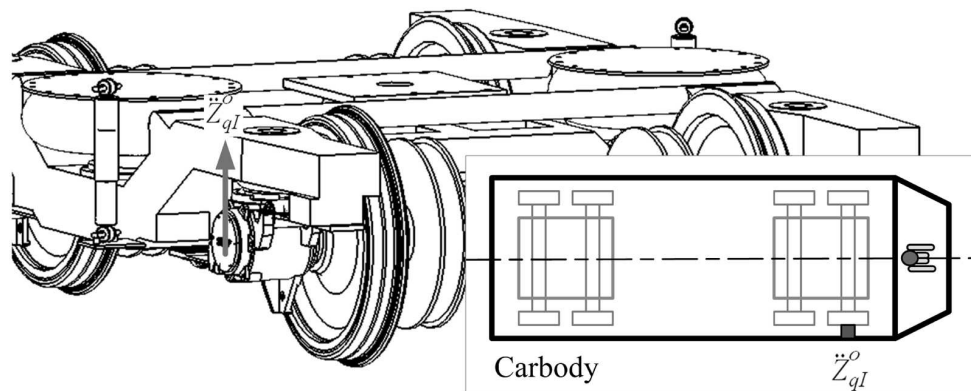
Review Only

1  
2  
3  
4  
5  
6  
7  
8  
9  
10  
11  
12  
13  
14  
15  
16  
17  
18  
19  
20  
21  
22  
23  
24  
25  
26  
27  
28  
29  
30  
31  
32  
33  
34  
35  
36  
37  
38  
39  
40  
41  
42  
43  
44  
45  
46  
47  
48  
49  
50  
51  
52  
53  
54  
55  
56  
57  
58  
59  
60



139x64mm (600 x 600 DPI)

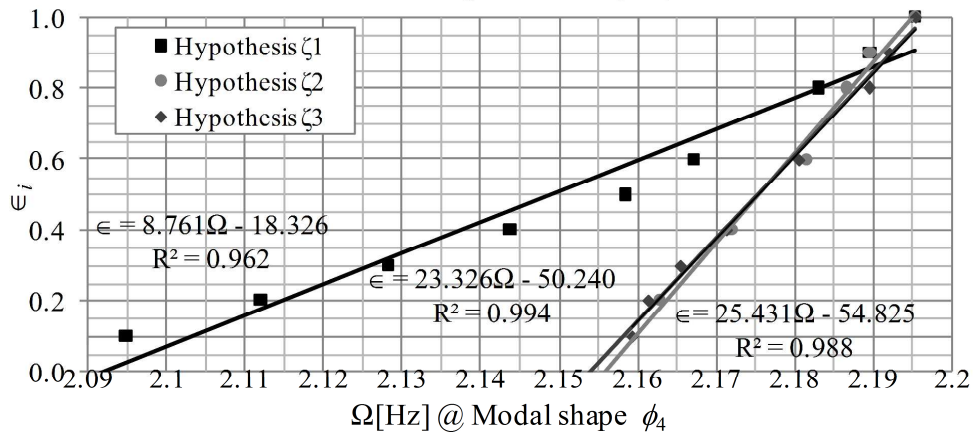
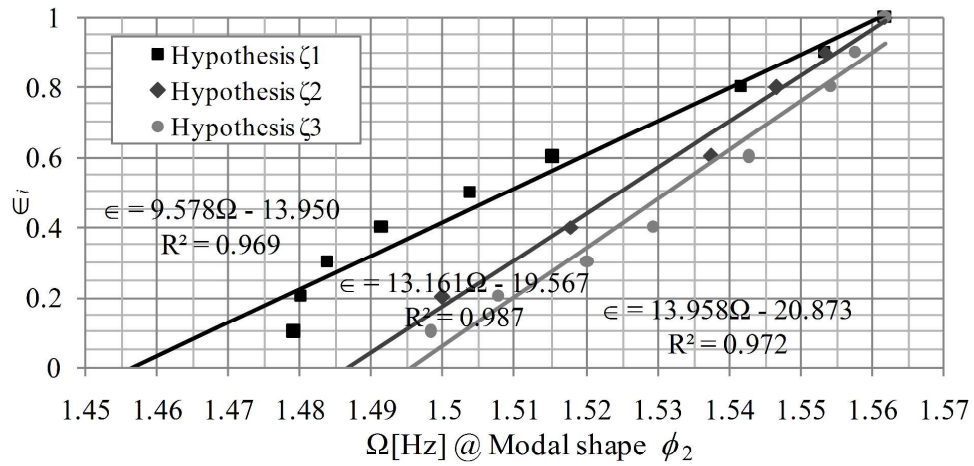
1  
2  
3  
4  
5  
6  
7  
8  
9  
10  
11  
12  
13  
14  
15  
16  
17  
18  
19  
20  
21  
22  
23  
24  
25  
26  
27  
28  
29  
30  
31  
32  
33  
34  
35  
36  
37  
38  
39  
40  
41  
42  
43  
44  
45  
46  
47  
48  
49  
50  
51  
52  
53  
54  
55  
56  
57  
58  
59  
60



(c)

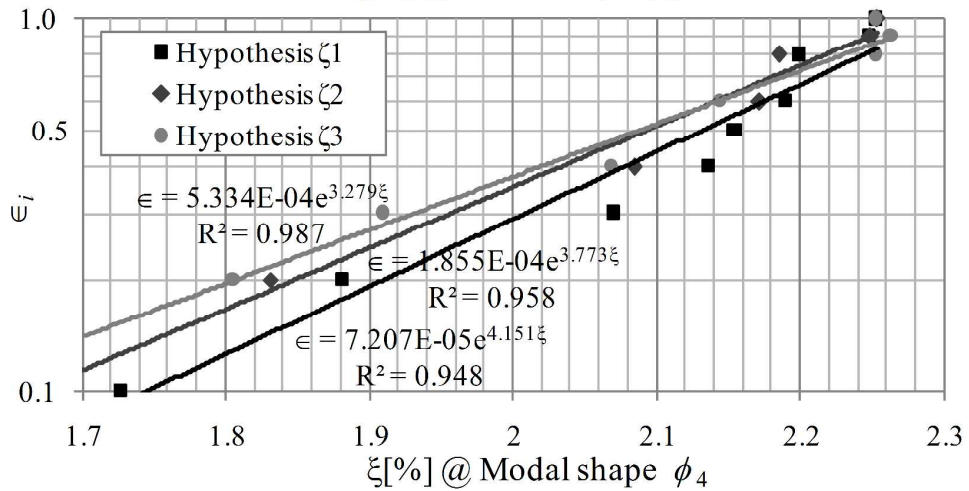
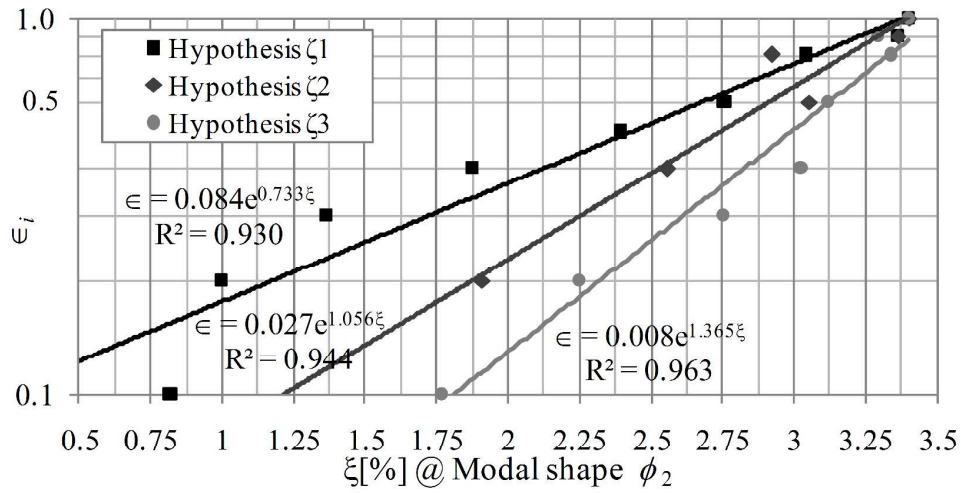
139x59mm (600 x 600 DPI)

er Review Only



167x151mm (600 x 600 DPI)

Only

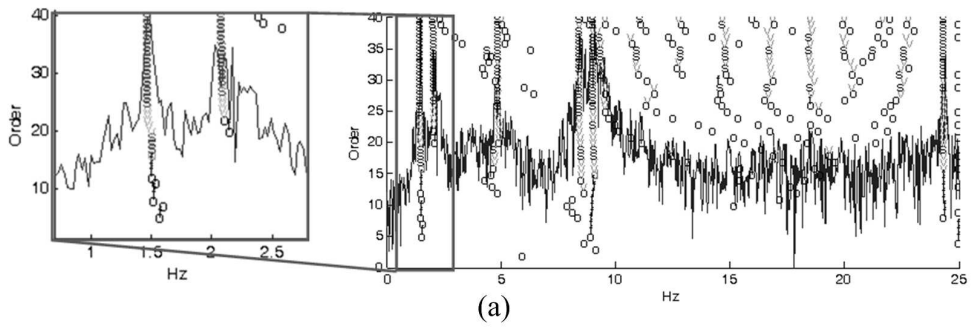


143x141mm (600 x 600 DPI)

Only

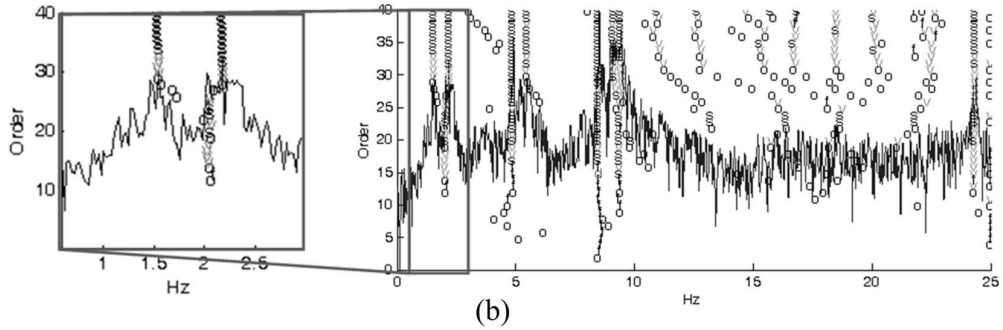


1  
2  
3  
4  
5  
6  
7  
8  
9  
10  
11  
12  
13  
14  
15  
16  
17  
18  
19  
20  
21  
22  
23  
24  
25  
26  
27  
28  
29  
30  
31  
32  
33  
34  
35  
36  
37  
38  
39  
40  
41  
42  
43  
44  
45  
46  
47  
48  
49  
50  
51  
52  
53  
54  
55  
56  
57  
58  
59  
60



139x45mm (600 x 600 DPI)

Peer Review Only

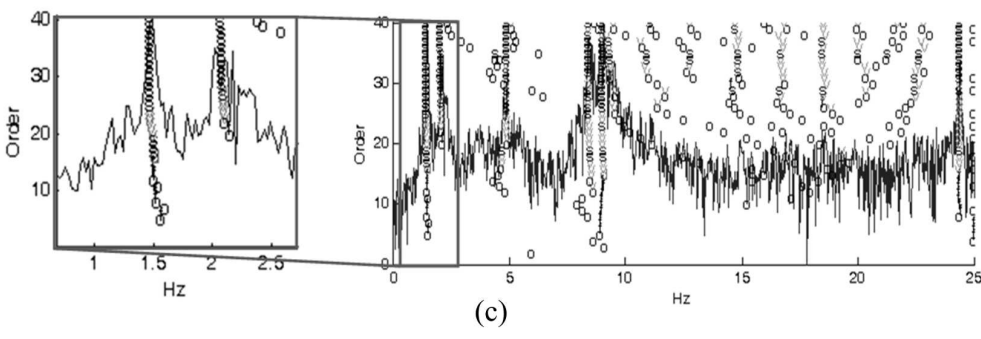


140x46mm (600 x 600 DPI)

Peer Review Only

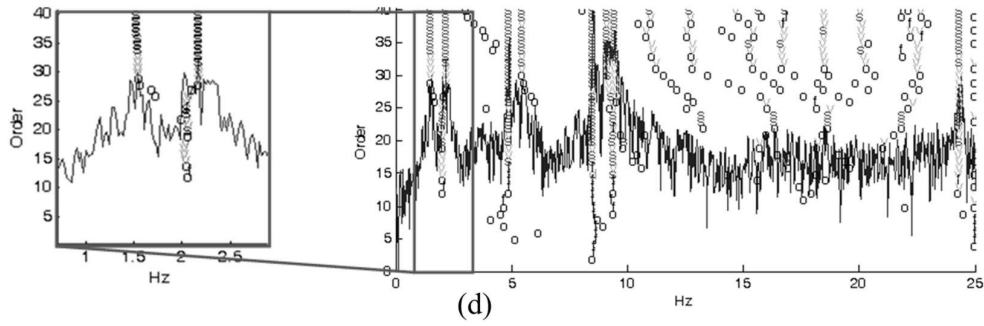
1  
2  
3  
4  
5  
6  
7  
8  
9  
10  
11  
12  
13  
14  
15  
16  
17  
18  
19  
20  
21  
22  
23  
24  
25  
26  
27  
28  
29  
30  
31  
32  
33  
34  
35  
36  
37  
38  
39  
40  
41  
42  
43  
44  
45  
46  
47  
48  
49  
50  
51  
52  
53  
54  
55  
56  
57  
58  
59  
60

1  
2  
3  
4  
5  
6  
7  
8  
9  
10  
11  
12  
13  
14  
15  
16  
17  
18  
19  
20  
21  
22  
23  
24  
25  
26  
27  
28  
29  
30  
31  
32  
33  
34  
35  
36  
37  
38  
39  
40  
41  
42  
43  
44  
45  
46  
47  
48  
49  
50  
51  
52  
53  
54  
55  
56  
57  
58  
59  
60



139x46mm (600 x 600 DPI)

Peer Review Only

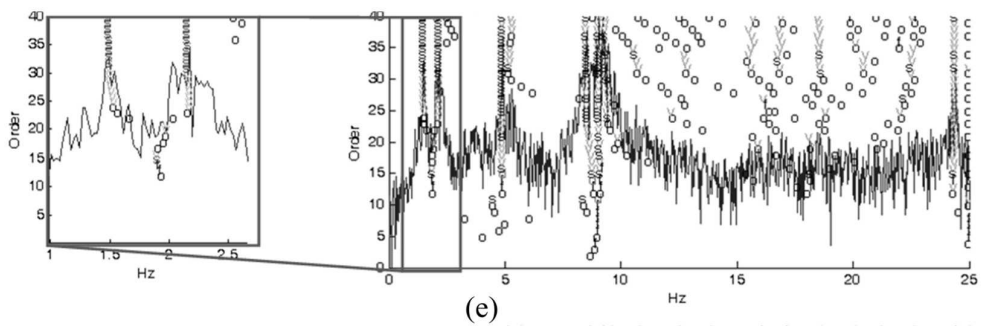


140x45mm (600 x 600 DPI)

Peer Review Only

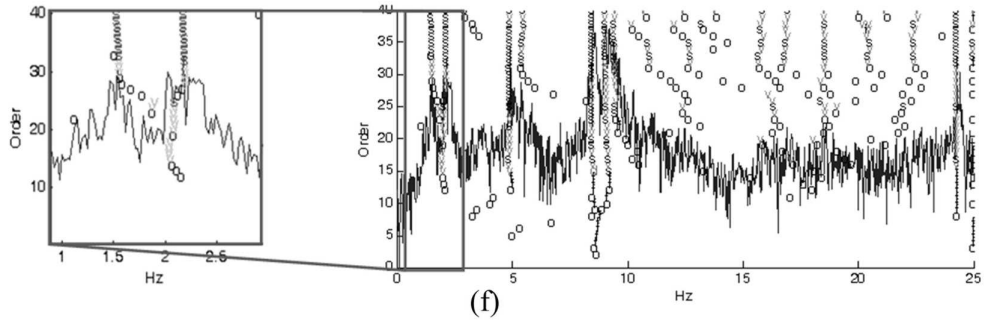
1  
2  
3  
4  
5  
6  
7  
8  
9  
10  
11  
12  
13  
14  
15  
16  
17  
18  
19  
20  
21  
22  
23  
24  
25  
26  
27  
28  
29  
30  
31  
32  
33  
34  
35  
36  
37  
38  
39  
40  
41  
42  
43  
44  
45  
46  
47  
48  
49  
50  
51  
52  
53  
54  
55  
56  
57  
58  
59  
60

1  
2  
3  
4  
5  
6  
7  
8  
9  
10  
11  
12  
13  
14  
15  
16  
17  
18  
19  
20  
21  
22  
23  
24  
25  
26  
27  
28  
29  
30  
31  
32  
33  
34  
35  
36  
37  
38  
39  
40  
41  
42  
43  
44  
45  
46  
47  
48  
49  
50  
51  
52  
53  
54  
55  
56  
57  
58  
59  
60



140x44mm (600 x 600 DPI)

Peer Review Only



141x45mm (600 x 600 DPI)

Peer Review Only

1  
2  
3  
4  
5  
6  
7  
8  
9  
10  
11  
12  
13  
14  
15  
16  
17  
18  
19  
20  
21  
22  
23  
24  
25  
26  
27  
28  
29  
30  
31  
32  
33  
34  
35  
36  
37  
38  
39  
40  
41  
42  
43  
44  
45  
46  
47  
48  
49  
50  
51  
52  
53  
54  
55  
56  
57  
58  
59  
60